



### Conference Paper

## **Kinematic Analysis and Comparison of Wheeled Locomotion Performance**

**Author(s):**

Thueer, Thomas; Siegwart, Roland

**Publication Date:**

2008

**Permanent Link:**

<https://doi.org/10.3929/ethz-a-010034615> →

**Rights / License:**

[In Copyright - Non-Commercial Use Permitted](#) →

This page was generated automatically upon download from the [ETH Zurich Research Collection](#). For more information please consult the [Terms of use](#).

# Kinematic Analysis and Comparison of Wheeled Locomotion Performance

Thomas Thueer and Roland Siegwart

Autonomous Systems Lab, ETH Zurich

CLA E18, Tannenstrasse 3

8092 Zurich, Switzerland

{ thomas.thueer, roland.siegwart } @ mavt.ethz.ch

## ABSTRACT

*Selection of a suspension mechanism for a rough terrain robot depends on many parameters. A proper comparison based on well defined metrics is indispensable. This paper follows the line of previous work and extends the list of investigated aspects by a kinematical analysis. A metric is defined that indicates the risk of violation of kinematically imposed constraints on rough terrain. A comparison of several rovers based on this metric is described and the validity of this theoretical metric for real world performance is shown by means of hardware measurements.*

**Keywords:** Locomotion performance, comparison, kinematic analysis, metrics, exploration rover.

## INTRODUCTION

For every planetary exploration mission specific requirements have to be defined based on which the most appropriate suspension configuration can be selected. In the case of the ExoMars mission trade-offs were made and the selection process was completed with the design of the prototypes. However, future missions might require rovers with different capabilities. Therefore, performance evaluation of wheeled locomotion systems remains an important issue.

This paper follows the line of previous work which aims at comparing suspension configurations based on different metrics. The focus is on simple models which allow for fast modeling and simulation with little processing power. The idea is not to produce the most accurate simulations possible but to provide tools that can be used in the early phases of a project when information about the final system is sparse and the number of candidate systems is big.

In [1] a tool is presented that was developed in the frame of ESA's Rover Chassis Evaluation Tools (RCET) activity. [2] and [3] describe how this tool was used to determine the obstacle climbing capabilities and the stability of different rover chassis configurations. Further work included the validation of the simulation results through real hardware testing [4] which showed the usefulness of the tool. In order to evaluate additional parameters, new metrics were defined. In [5] the compliance of the suspension with kinematical constraints imposed by the terrain was investigated. The simulation results predicted significant differences between the analyzed systems. The present work completes this study by means of experimental testing of real rovers.

Several people have presented work that focused on kinematics for different purposes. Forward kinematics was used in simulation for the estimation of rover position and heading in [6]. Wheel actuation commands can be derived for a desired rover motion by means of an inverse kinematics model [7]. [8] and [9] included rover kinematics in the estimation of the wheel-ground contact angles and [10] developed a kinematic observer for articulated rovers.

A kinematic model can provide valuable information because the ability of articulated rovers to adapt to uneven terrain makes it difficult to relate rover motion to wheel motion and requires the wheels to move at different speeds. In this context rover control plays a central role. Several control strategies have been presented which aim at increasing the rover's performance by synchronizing wheel velocities [11], setting optimal torques depending on the rover's state [12, 13] or actively adapting the rover's configuration based on kinematic information [14].

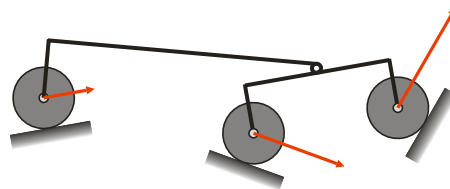


**Fig. 1.** Example of wheel speeds imposed by kinematic constraints in rough terrain.

Contrary to the referenced examples, where kinematics was used during simulation or operation of a rover, kinematic properties were analyzed in this work to evaluate the performance potential of selected systems. In rough terrain, the speeds imposed by the kinematic properties of the suspension are different on all wheels given that negative effects like slip are to be avoided. Fig. 1 shows that the ideal velocities on the wheels differ significantly. The bigger this difference, the more difficult it is to satisfy the constraints. Violation of such constraints induces slip. Therefore, the selected rovers were analyzed with regards to their ideal velocity distribution that is an indicator for the risk of slip during motion in uneven terrain.



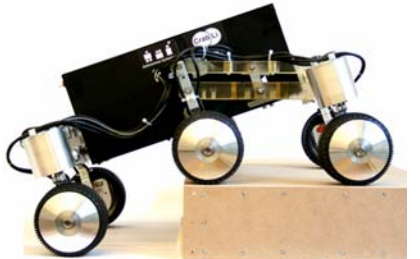
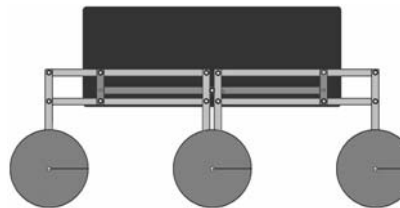
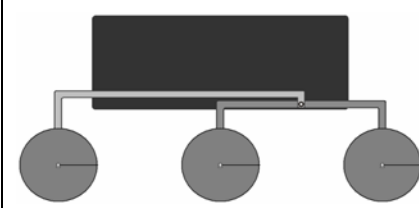
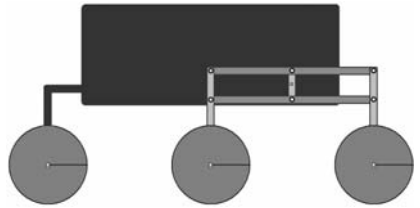
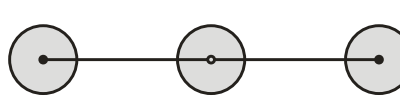
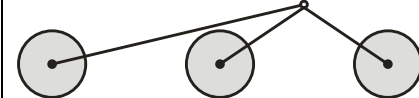
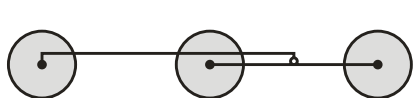
In the next section, the evaluated systems are presented before the kinematic modeling is described. Then, the performance metrics and the simulation setup are introduced. Finally, the results from hardware testing are compared to the predictions from simulation.

## SUSPENSION SYSTEMS AND KINEMATIC MODELS

In this section the analyzed rovers are briefly presented and the kinematic modeling is explained. For reasons of consistency, the same rovers were selected for the kinematic analysis as in [4] where more details can be found about the systems. However, a new, modular hardware platform was developed which allows for configuration of four different suspension types: the selection consisting of CRAB [15] and RCL-E [16] was extended by the configurations of NASA's rocker bogie (RB) suspension [17] and ESA's ExoMars rover [18]. It is important to point out that the behavior of RB and ExoMars is identical in 2D which also applies to the kinematic models used in this work. Therefore, only three configurations are listed in Table 1 where different representations of the rovers can be found: photo of the hardware, simulation model, and kinematic model. The kinematic models were simplified such that they correctly represent the mechanical system and maintain identical behavior like the real rovers but modeling of parallel structures could be avoided.

Since the focus of this work was the comparison of suspension types and not of the original rovers, the hardware was designed in a way that the main parameters remained the same when the configurations were changed. The resulting modular system has a total mass of ~18 kg, wheels with a diameter of 0.11 m, a foot print of 0.456 m and the CoG in the middle of the rover close to the body's base plate. These common dimensions allow for a proper comparison of the suspension types regardless of terrain characteristics.

**Table 1.** Different representations of the evaluated systems: breadboard, simulation model, kinematic model.

CRAB Autonomous Systems Lab  Symmetric structure based on four parallel bogies, differential mechanism	Rocker bogie (ExoMars*) NASA / JPL  Rocker with pivot to connect bogie, differential mechanism	RCL-E RCL / ESA  Two parallel bogies at side/front, one transversal parallel bogie at rear, no differential
		
		
		

(\* Due to identical structure and behavior in 2D, the results of RB are also valid for ExoMars.)

Rough-terrain robots make use of a suspension mechanism that consists of several rigid elements connected through joints of a certain number of degrees of freedom (DoF) resulting in a structure that has one system DoF. This enables the rovers to move along uneven terrain without losing contact with the ground. Basic kinematics was used to represent these characteristics and set up the rover models. The modeling process is explained by the example of RB as it is depicted in Fig. 2.

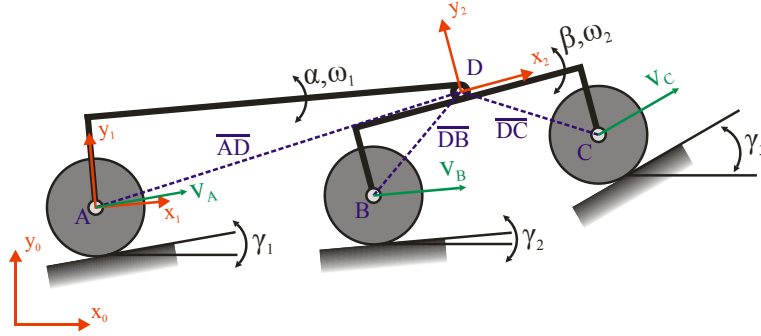


**Fig. 2.** Kinematic model of RB.

The system is defined through the vectors of constant length  $AD$ ,  $DB$ , and  $DC$ , the wheel-ground contact angles ( $\gamma_i$ ) as well as the orientation of rocker ( $\alpha$ ) and bogie ( $\beta$ ) with respect to the inertial system. In reality  $\alpha$  can be measured by means of an inertial measurement unit (IMU) and  $\beta$  with an angular sensor in  $D$  that measures the relative movement between rocker and bogie. Measuring the wheel-ground contact angles requires tactile wheels as in [13] and [19].

The unknown parameters are the magnitudes of the velocities in  $A$ ,  $B$ ,  $C$ , and  $D$  (given that the wheels always touch the ground) as well as the rotational velocities of rocker ( $\omega_1$ ) and bogie ( $\omega_2$ ). The velocity in  $D$  is not of interest; therefore it is expressed by means of the other velocities yielding an equation system with four equations (2D) and five unknowns. As it was mentioned before, rovers have one DoF which means that one velocity can be chosen as input. Thus, the equation system has exactly one solution. First,  $v_D$  is expressed in inertial system coordinates through  $A$ ,  $B$ , and  $C$ .

$$\mathcal{G}_{D/A} := \mathcal{G}_D = \mathcal{G}_A + \omega_1 \times {}^0R(\alpha) {}^1\overline{AD} \quad (1)$$

$$\mathcal{G}_{D/B} := \mathcal{G}_D = \mathcal{G}_B + \omega_2 \times {}^2R(\beta) {}^2\overline{DB} \quad (2)$$

$$\mathcal{G}_{D/C} := \mathcal{G}_D = \mathcal{G}_C + \omega_2 \times {}^2R(\beta) {}^2\overline{DC} \quad (3)$$

with  $v_i$  = velocity in  $i$  w.r.t. inertial system,  
 $\omega_i$  = rotational velocity of system  $i$  w.r.t. inertial system,  
 ${}_j^iR(m)$  = transformation from system  $j$  to  $i$  by rotation of angle  $m$ ,  
 ${}_i\overline{XY}$  = vector from  $X$  to  $Y$  expressed in coordinate system  $i$ .

(1)-(3) are rearranged to:

$$v_{D/A} = v_{D/B}; v_{D/A} = v_{D/C} \quad (4)$$

Then, the equation system can be written as

$$Ax = b \text{ with } x = (v_B, v_C, \omega_1, \omega_2)^T \quad (5)$$

(5) can be solved for  $x$  with  $v_A$  as input. If the velocity input is given at  $B$  or  $C$  the system has to be transformed accordingly. Models of the same form were also generated for CRAB and RCL-E. Since the kinematic model takes only one input velocity, special attention has to be paid to the selection of the reference where this input is set.

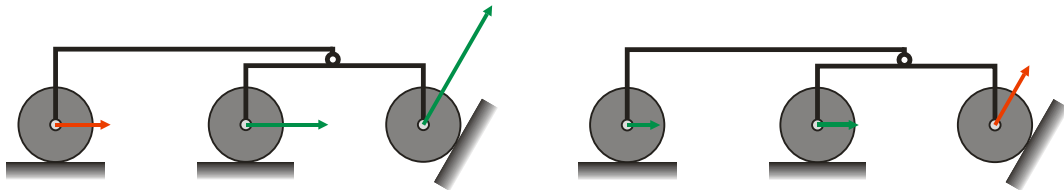


**Fig. 3.** Velocity distribution for different reference wheels.

In Fig. 3, RB is depicted twice in the same position but with different reference wheels. The velocity of the reference wheel is the same in both cases (red flash). The green flashes indicate the corresponding ideal velocities on the other wheels. While the ratio between the velocities of the wheels remains the same in both cases, the effective required velocity per wheel varies greatly. This issue will be considered in the formulation of the respective metric.

## PERFORMANCE METRICS

The definition of metrics is indispensable if the performance of a system is to be evaluated. It has to be defined what is considered good or bad performance if a system reaches a certain value w.r.t. a given metric.

### Slip

Two different definitions of slip are used in this work. The first definition reflects the instantaneous slip  $s$  [-] as difference between theoretical velocity due to wheel rotation  $\theta$  and effective traveling speed  $v$ .

$$s = \frac{r\dot{\theta} - v}{r\dot{\theta}} \quad (6)$$

The second definition is used to express the total distance  $s_{tot}$  [m] a wheel slipped during a full test run. The absolute value of slip is used to include all sliding motions.

$$s_{tot} = \sum_{j=1}^m \sum_{i=1}^n \left| \Delta pos_{enc_{i,j}} - \Delta pos_{wc_{i,j}} \right| \quad (7)$$

with  $m$  = number of measurements,  $n$  = number of wheels,  $\Delta pos_{wc}$  = effective displacement and  $\Delta pos_{enc}$  = measured displacement based on wheel rotation. Slip is bad for the odometry and a waste of energy because it does not contribute to the movement of the rover. Therefore, slip must be small for good performance.

In this work, slip could only be used as a metric in simulation because the necessary measurement devices to determine  $\Delta pos_{wc}$  were not available for hardware testing.

### Velocity Constraint Violation (VCV)

$VCV$  [-] is a measure for the risk of violating kinematic constraints through deviation of each wheel from the ideal velocity and should therefore be as small as possible. In the case of the commonly used constant velocity control, deviation from the ideal velocity is inevitable in uneven terrain and leads to slip.  $VCV$  is an indicator of how good a suspension system is able to adapt to the terrain. First,  $V$  is defined for each wheel as the ratio between ideal velocity  $v_{kin}$  and reference velocity  $v$ .

$$V = \frac{v_{kin}}{v} \quad (8)$$

Since positive and negative deviations tend to even out the mean value of  $V$  over a full test run with  $n$  measurements, the standard deviation is used instead.

$$\sigma_V = \left( \frac{1}{n} \sum_{i=1}^n (V_i - \bar{V})^2 \right)^{\frac{1}{2}} \quad (9)$$

For an  $m$ -wheel robot  $((m-1) \cdot m)$  values of  $V$  can be calculated. On the one hand,  $V$  is always 1 at the reference wheel and can be neglected  $(m-1)$ . On the other hand,  $v_{kin}$  is highly dependent on the selection of the reference wheel. Thus,  $V$  has to be calculated for each of the  $m$  wheels as reference. Therefore,  $VCV$  is defined as the mean value over all  $\sigma_V$ .

$$VCV = \frac{1}{m(m-1)} \sum_{j=1}^m \sum_{i=1}^{m-1} (\sigma_V)_{i,j} \quad (10)$$

Since  $VCV$  is a metric for theoretical performance analysis, it is used in simulation only.



### Mean Torque ( $\bar{T}$ )

The mean torque,  $\bar{T}$  [Nm], is used as parameter for validation of the  $VCV$  metric. It is calculated as the mean torque value over a full test run. The wheel torque,  $T_w$ , can be derived from the current measurements by the motor controllers.

$$T_w = I \cdot k_T \cdot \eta \cdot n / 1000 \quad (11)$$

with  $I$  = current [A],  $k_T$  = torque constant [mNm/A],  $\eta$  = efficiency of gearbox [-] and  $n$  = reduction ratio of gearbox [-].

### SIMULATION SETUP

The simulation tool, Working Model 2D (WM2D) by Design-Simulation, was selected because of its ease of use to set up dynamic models, its capability to do collision detection and the possibility to be interfaced with Matlab. Fig. 4 depicts the distribution of tasks and the interface between the programs. WM2D handles the dynamic model of the rover and simulates it on a given terrain. The motor model was implemented in Matlab where the motor controller is running as well as the kinematic model.

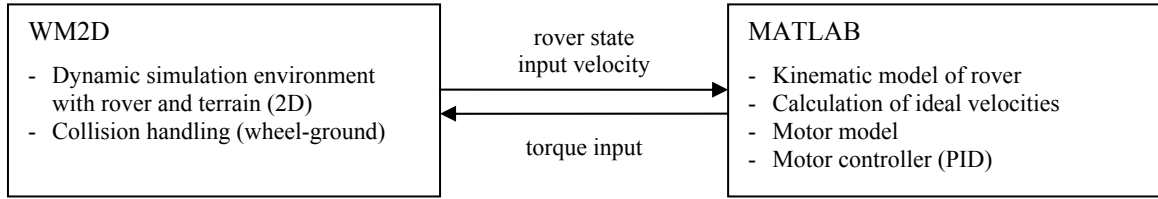


**Fig. 4.** Overview of tasks handled by WM2D and Matlab.

### CORRELATION BETWEEN SIMULATION AND HARDWARE

All systems were simulated and tested under identical conditions. The wheel speed was set to 0.04 m/s. Rough terrain was simulated by means of two sinusoidal bumps as shown in (Fig. 5).

The results from the kinematic analysis are listed in Table 2. The standard deviation of  $V$  is given for each wheel and all three reference wheel cases. While  $\sigma_V$  of CRAB and RCL-E is between 0.06 and 0.14, it reaches values of 0.27 for the RB. It is noticeable that the high values are always linked to the rear wheel of RB. The most likely explanation for these results is that the distance between rear wheel and bogie wheels of the RB varies greatly in rough terrain depending on the state of the rover. To enable these changes the ideal velocities differ significantly leading to high  $\sigma_V$ . This is also reflected in the metric  $VCV$ . The performance of CRAB and RCL-E is similar while the performance of RB is strikingly inferior.

To confirm that  $VCV$  is an indicator for kinematic constraint violation in the form of slip, Fig. 6 depicts the simulation results for instantaneous slip  $s$  and total accumulated slip  $s_{tot}$  over the full test run. The numerical values of  $s_{tot}$  are given in Table 3. As predicted with the  $VCV$  metric, CRAB and RCL-E clearly outperform RB with only about 2/3 of the total slip. The graphs for  $s$  show that CRAB and RCL-E adapt well to the terrain causing little slip. The slip curve of RB confirms the assumption that the problem stems from the varying distance between rear wheel and bogie wheels. The peaks correspond to the situations where big state changes are needed to adapt to the terrain.

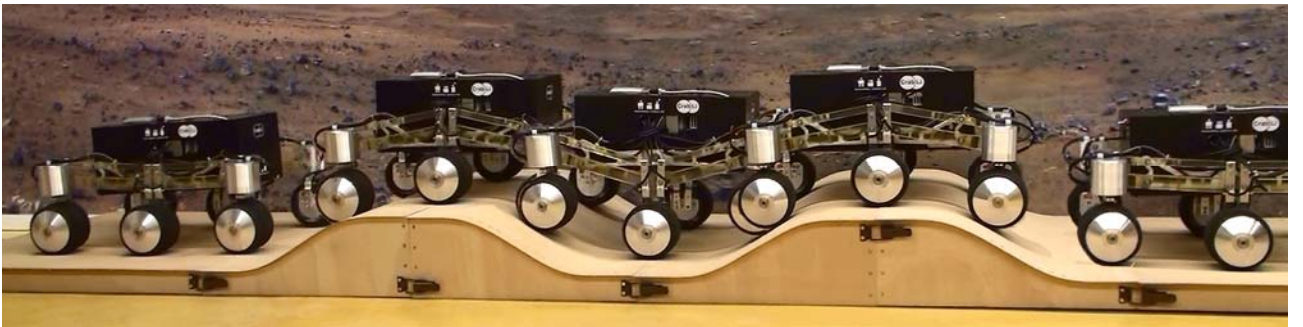


**Fig. 5.** Test run of CRAB configuration on sinusoidal test terrain.

**Table 2.** Simulation results for metric  $VCV$ .

rover	$\sigma_V$						$VCV [-]$	(%)
	wheel	ref. rear	wheel	ref. middle	wheel	ref. front		
<b>CRAB</b>	middle	0.11	rear	0.09	rear	0.11	<b>0.11</b>	<b>59</b>
	front	0.11	front	0.09	middle	0.12		
<b>RCL-E</b>	middle	0.14	rear	0.10	rear	0.09	<b>0.09</b>	<b>53</b>
	front	0.10	front	0.06	middle	0.07		
<b>RB/ExoMars</b>	middle	0.27	rear	0.20	rear	0.20	<b>0.18</b>	<b>100</b>
	front	0.26	front	0.06	middle	0.07		

**Table 3.** Absolute accumulated slip  $s_{tot}$ .

	<b>CRAB</b>	<b>RCL-E</b>	<b>RB/ExoMars</b>
<b>absolute slip accumulated [m]</b>	0.43	0.43	0.67
<b>(%)</b>	64	64	100

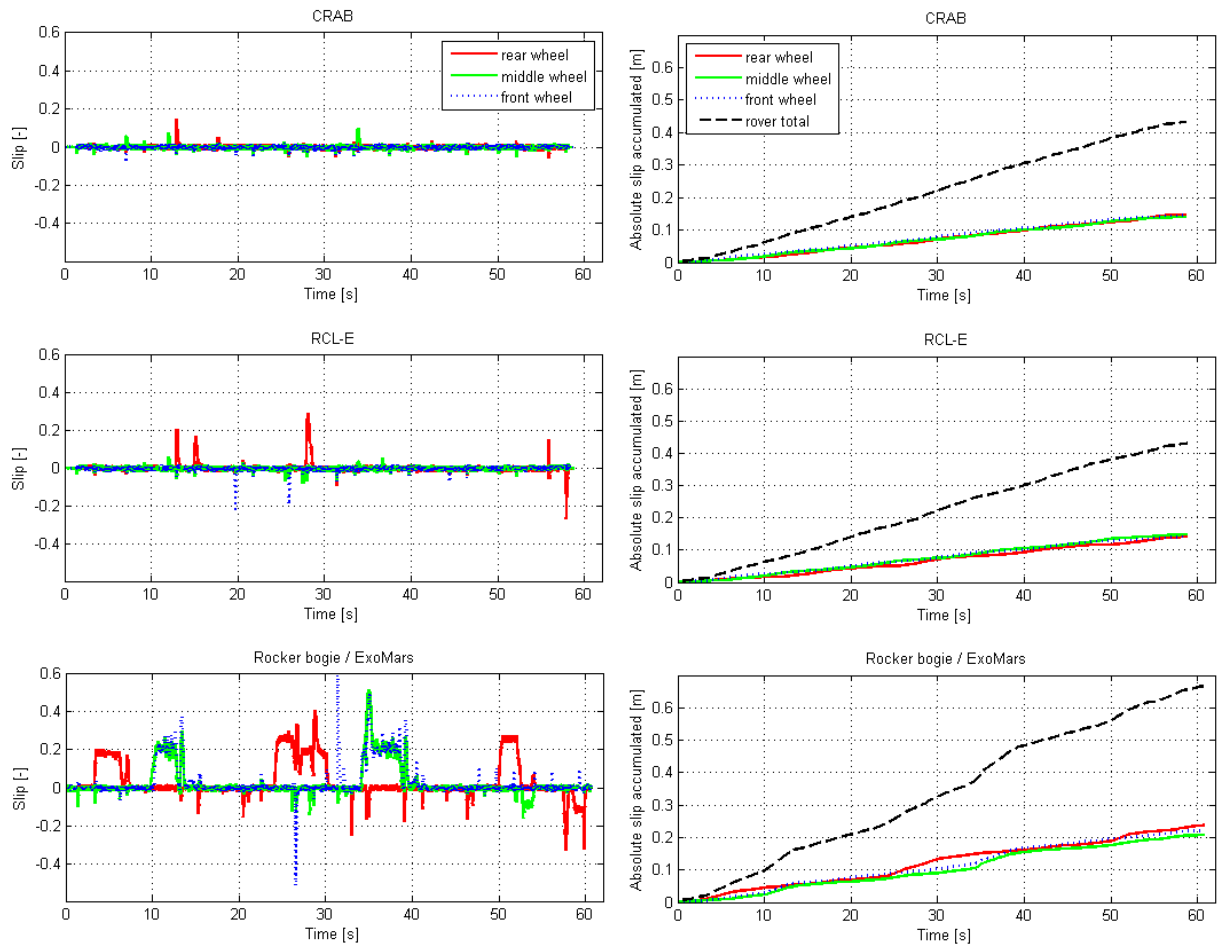


**Fig. 6.** Simulation results for metric slip:  $s$  (left),  $s_{tot}$  (right).

In simulation, the full state of the rover is always known, thus, wheel position and rotation can be accessed at every time step to calculate slip. The available test setup, however, was not capable of providing this information. Thus, the main challenge of the validation was to detect the occurrence of slip and quantify it by use of other parameters.

Slip occurs when kinematic constraints are broken. For this, the traction force has to exceed the resisting friction force which is only possible if the motor torque is big enough. This means, that each time excessive slip occurs, the torque values have to be higher than actually needed by the rover for the pure displacement, increasing the average torque over

a full test run. Therefore, the torque measurements were used as an indicator for slip in order to validate the  $VCV$  metric.

It was stated before that slip is a loss of energy. Therefore, it would have been interesting to measure the mean power consumption of the different configurations. Unfortunately, the breadboard does not dispose of a power measurement device and the current information from the motor controllers is not suited to calculate power accurately because the signals to the motors are pulse-width modulated (PWM). This means for electrical power calculation ( $P=U I$ ) that the current is known but not the actual voltage, and for mechanical power ( $P=T \omega$ ) that the time span during which the torque is applied is unknown. Thus, the mean torque value is a good alternative measure because it does not include the notion of time which eliminates the PWM problem.

Fig. 7 depicts the measured wheel torques of all suspension configurations. The shapes of the torque curves correspond very well to the slip curves in Fig. 6. Low torques are required by CRAB and RCL-E, and no noticeable peaks occur. The curves of RB's torques show the same peaks as the corresponding slip curves, confirming that slip occurs also in reality.

In Table 4, the first row contains the average measured absolute torque of all wheels on the left side (comparison with 2D model); the relative performance between the rovers is given in the second row. The respective  $VCV$  values in rows three and four are provided for comparison. The numerical correlation of the relative performance in reality and simulation is very satisfying. The  $VCV$  values predict similar performance of CRAB and RCL-E, more than 40% better than RB. The measurements found  $\bar{T}$  of 0.33 Nm and 0.3 Nm for CRAB and RCL-E respectively which is approximately 40% better than the mean torque of RB at 0.51 Nm.

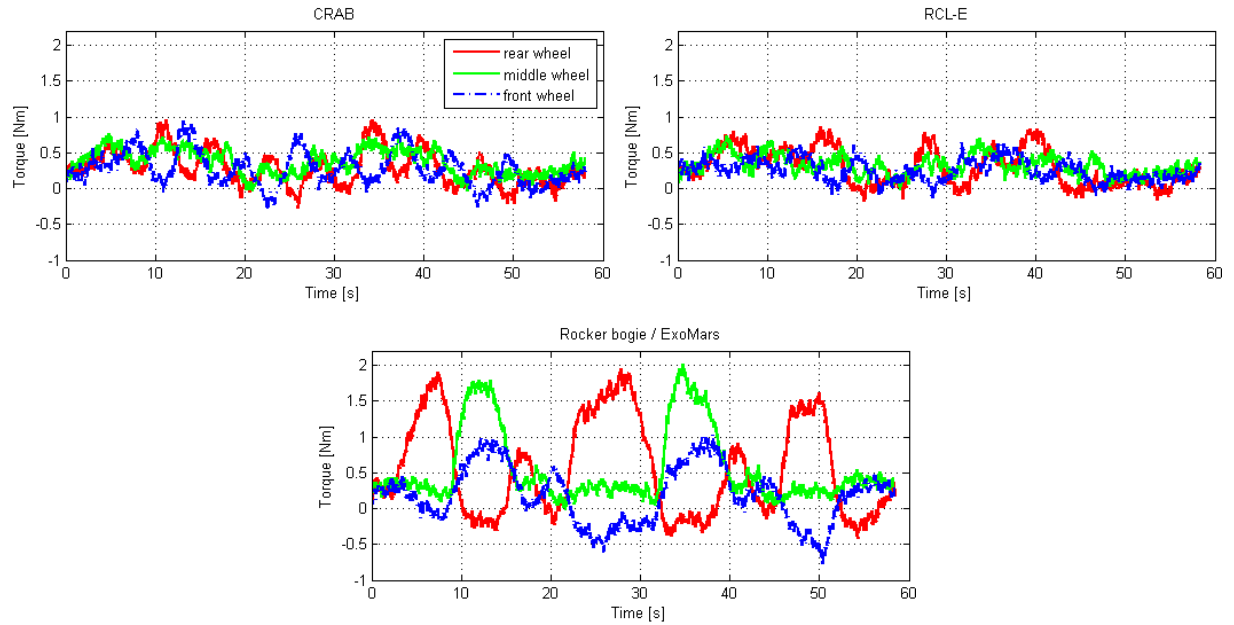


**Fig. 7.** Wheel torque measurements. Since the terrain was designed such that the behavior of the rover can be treated as 2D, like in simulation, the measurements from both sides of the rover are identical. Thus, only one set of measurements is shown in the graphs.

**Table 4.** Mean torque and  $VCV$ .

	CRAB	RCL-E	RB/ExoMars
mean torque [Nm]	0.33	0.3	0.51
(%)	64	58	100
$VCV$ [-]	0.11	0.09	0.18
(%)	59	53	100



## CONCLUSION

Selection of a rover suspension configuration depends on the requirements for a specific application. Therefore, it is useful to have a big number of different metrics. This paper presented the new metric  $VCV$  which is an indicator for the rover's capability to adapt to uneven terrain without violating kinematic velocity constraints. A high value of  $VCV$  indicates a big risk of slip which is not only bad for odometry but also leads to increased energy consumption. Since  $VCV$  is a theoretical value, this work aimed at relating the metric to real world parameters. The results from simulation and hardware testing show a very good correlation between  $VCV$ , slip and mean torque. It was shown in simulation that CRAB and RCL-E perform better on the test terrain with low  $VCV$  values compared to RB. This difference in performance is reflected in reality in the measured required mean torque which proves the  $VCV$  metric to be very valuable for performance comparison.

## ACKNOWLEDGEMENTS

This work was support by the European Space Agency through contract no. 18191/04/NL/PM - Mars Rover Chassis. Thanks to Markus Bühler, Dario Fenner, Cunégonde, and Stefan Bertschi for hardware support and Mark Hoepfflinger for the development of the GUI.

## REFERENCES

- [1] A. Krebs, T. Thueer, S. Michaud, and R. Siegwart, "Performance Optimization for Passive Rover Structure: A 2D Quasi-Static Tool," in *IEEE International Conference on Intelligent Robots and Systems (IROS'06)*, Beijing, China, 2006.
- [2] T. Thueer, A. Krebs, and R. Siegwart, "Comprehensive Locomotion Performance Evaluation of All-Terrain Robots," in *IEEE International Conference on Intelligent Robots and Systems (IROS'06)*, Beijing, China, 2006.
- [3] S. Michaud, L. Richter, T. Thueer, A. Gibbesch, N. Patel, T. Huelsing, L. Joudrier, R. Siegwart, and B. Schaefer, "Rover Chassis Evaluation and Design Optimisation Using the RCET," in *The 9th ESA Workshop on Advanced Space Technologies for Robotics and Automation (ASTRA'06)*, Noordwijk, The Netherlands, 2006.
- [4] T. Thueer, A. Krebs, P. Lamon, and R. Siegwart, "Performance Comparison of Rough-Terrain Robots – Simulation and Hardware," *International Journal of Field Robotics (Special Issue on Space Robotics)*, Wiley, vol. 24, pp. 251 - 271, March 2007.
- [5] T. Thueer and R. Siegwart, "Characterization and Comparison of Rover Locomotion Performance Based on Kinematic Aspects," in *International Conference on Field and Service Robotics (FSR2007)*, Chamonix, France, 2007.
- [6] H. Hacot, S. Dubowsky, and P. Bidaud, "Analysis and Simulation of a Rocker-Bogie Exploration Rover," in *CISM-IFTOMM Symposium*, Paris, France, 1998.
- [7] M. Tarokh, G. McDermott, S. Hayati, and J. Hung, "Kinematic Modeling of a High Mobility Mars Rover," in *IEEE International Conference on Robotics and Automation (ICRA'99)*, Detroit, Michigan, USA, 1999, pp. 992-998 vol.2.
- [8] K. Iagnemma and S. Dubowsky, "Vehicle Wheel-Ground Contact Angle Estimation: with Application to Mobile Robot Traction Control," in *International Symposium on Advances in Robot Kinematics (ARK '00)*, 2000.
- [9] T. Peynot and S. Lacroix, "Enhanced locomotion control for a planetary rover," in *IEEE International Conference on Intelligent Robots and Systems (IROS'03)*, Las Vegas, USA, 2003, pp. 311-316 vol.1.
- [10] J. Balaram, "Kinematic State Estimation for a Mars Rover," *Robotica*, vol. 18, p. 12, 2000.
- [11] E. T. Baumgartner, H. Aghazarian, and A. Trebi-Ollennu, "Rover Localization Results for the FIDO Rover," in *SPIE Proc. Vol. 4571, Sensor Fusion and Decentralized Control in Autonomous Robotic Systems IV*, Newton, MA, USA, 2001.
- [12] P. Lamon and R. Siegwart, "Wheel Torque Control in Rough Terrain - Modeling and Simulation," in *IEEE International Conference on Robotics and Automation (ICRA'05)*, Barcelona, Spain, 2005, p. 6.
- [13] A. Krebs, T. Thueer, E. Carrasco, and R. Siegwart, "Towards torque control of the CRAB rover," in *International Symposium on Artificial Intelligence, Robotics and Automation in Space (i-SAIRAS)*, Pasadena, USA, 2008.
- [14] C. Grand, F. B. Amar, and P. Bidaud, "Kinematic analysis and stability optimization of a reconfigurable legged-wheeled mini-rover," in *Unmanned Ground Vehicle Technology IV*, Orlando, FL, USA, 2002, pp. 295-302.
- [15] T. Thueer, P. Lamon, A. Krebs, and R. Siegwart, "CRAB - Exploration Rover with Advanced Obstacle Negotiation Capabilities," in *The 9th ESA Workshop on Advanced Space Technologies for Robotics and Automation (ASTRA'06)*, Noordwijk, The Netherlands, 2006.
- [16] V. Kucherenko, A. Bogatchev, and M. Van Winnendael, "Chassis Concepts for the ExoMars Rover," in *The 8th ESA Workshop on Advanced Space Technologies for Robotics and Automation (ASTRA'04)*, Noordwijk, The Netherlands, 2004.
- [17] R. Lindemann, "Dynamic Testing and Simulation of the Mars Exploration Rover," in *2005 ASME International Design Engineering Technical Conferences and*, Long Beach, USA, 2005.
- [18] S. Michaud, A. Gibbesch, T. Thueer, A. Krebs, C. Lee, B. Despont, B. Schaefer, and R. Slade, "Development of the ExoMars Chassis and Locomotion Subsystem," in *International Symposium on Artificial Intelligence, Robotics and Automation in Space (i-SAIRAS)*, Pasadena, USA, 2008.
- [19] M. Lauria, "New Locomotion Concepts For All-Terrain Robots (Nouveaux concepts de locomotion pour véhicules tout-terrain robotisés)," in *Autonomous Systems Lab*. vol. Ph.D. Lausanne, Switzerland: Ecole Polytechnique Fédérale de Lausanne (EPFL), 2003.